

1 **A pilot study exploring the effect of vehicular waste heat**

2 **on personal heat exposure**

3

4 Ashley Avila
5 School of Landscape Architecture and Planning
6 University of Arizona, Tucson, Arizona, USA

7
8 Nicole Iroz-Elardo
9 Department of Public Health Ethics, Advocacy and Leadership
10 Willamette University, Willamette, Oregon, USA

11
12 Kristina M. Currans
13 School of Landscape Architecture and Planning
14 University of Arizona, Tucson, Arizona, USA
15 Corresponding author

16
17 Ladd Keith
18 School of Landscape Architecture and Planning
19 University of Arizona, Tucson, Arizona, USA
20

21 **Abstract**

22 Understanding the causes of heat in various microclimates in cities is vital to
23 improving human thermal comfort and health in outdoor spaces. This pilot study uses an
24 experimental design to evaluate microclimate heat risk – including ambient air temperature
25 (TA) and wet bulb globe temperature (WBGT) – and approximate personal heat exposure of
26 people 1.5-3.0 meters (5-10 feet) away from idling vehicles. These measurements were taken
27 at a University of Arizona covered parking garage in June 2022 to investigate personal heat
28 exposure attributable to vehicular waste heat while also minimizing the effect of solar radiant
29 heat and wind. We used Kestrel 5400 devices to document the waste heat effects of a fleet of
30 six identical gasoline-powered vehicles on the surrounding microclimate by collecting TA,
31 wind velocity, and WBGT. When compared to the control, as well as comparing a period
32 when engines were not idling, we found a strong correlation between vehicle presence, TA,
33 and WBGT. Specifically, ordinary least-mean square (OLS) modeling shows an additional
34 TA per minute increase of 0.006°C (a 25% increase) per minute when the vehicles are on and
35 idling versus 0.024°C per minute increase that occurs from expected background morning
36 temperatures when the vehicle effect is removed. Until we transition to an electric fleet and
37 increase use of alternative modes of transportation, these findings can help inform how
38 transportation professionals design the built environment and manage traffic and transit
39 during summer months to prevent excessive heat exposure for pedestrians, cyclists, transit
40 riders, and other individuals near idling vehicles.

41 **Introduction**

42 Heat is an increasing climate risk for communities across the world. Extreme heat
43 events are occurring more frequently, are more intense, and are becoming longer in duration
44 due to climate change [1]. Heat wave frequency for cities in the United States (US) has

45 increased from an average of two heat waves per year in the 1960s to an average of six per
46 year in the 2010s [2]. Microclimates, or the climatic conditions in an immediate area, are
47 affected by multiple sources of heating and cooling, including waste heat, land cover,
48 evaporation, evapotranspiration, bodies of water, tree shade, and constructed object shade [3].
49 Variations in microclimate conditions can exacerbate personal heat exposure risk [3,4], and in
50 response, communities are increasingly planning for heat resilience by using both heat
51 mitigation strategies that reduce urban heat in the built environment and heat management
52 strategies that prepare and respond to chronic and acute heat risk [5,6]. The urban heat island
53 (UHI) effect is attributed to both heat that is absorbed in the built environment and then later
54 released, as well as waste heat [7].

55 Traditional gasoline-fueled vehicles reflect light, produce emissions, create noise, and
56 generate waste heat that increases heat in microclimates. Waste heat, or anthropogenic heat,
57 is released as a result of energy use from human activities and has been reported to cause a
58 1.0°C to 4.0°C (1.8°F to 7.2°F) warming in near-surface air temperatures [8]. By better
59 understanding the contribution of vehicular waste heat to microclimates, we can learn more
60 about heat's influence on travel behavior and heat resilience. Personal heat exposure, or the
61 human experience and perception of heat, is foundational to understanding how people
62 perceive and navigate outdoor spaces, including transportation spaces, particularly during
63 warm weather [4,9]. Studies have explored the effects of buildings and green space on their
64 respective microclimates, but an understudied area of work in planning is the effect of
65 vehicular waste heat on microclimates. This is likely due to the mobile nature of vehicles, the
66 variation in their operation, and the complexity of environmental conditions, resulting in
67 rapid changes in air temperature, solar radiation, and air movement [10].

68 The few studies that have addressed vehicular waste heat have hinted at a large impact
69 on the regional UHI. Waste heat loads tend to be largest during morning and evening peak

70 travel times. Analyzing the effects of vehicular, building, and human metabolism heat in the
71 summer suggests that heat from vehicles accounts for 47% to 62% of the total heat generated
72 [11]. Yet little research examines how vehicle waste heat reduces pedestrian perceived
73 comfort, a factor often cited in both traffic safety [12] and green facility contexts [13]. While
74 guidelines to provide systematic overviews of microclimate field measurements exist to
75 support research procedures in urban areas, more studies are needed to provide frameworks in
76 various climates and diverse conditions [14].

77 Heat severity is also inequitable felt. For instance, heat severity is higher in previously
78 redlined communities and those with higher proportions of minority or lower-income
79 households [15,16]. Yet, the effect of vehicles themselves on ground-level TA and personal
80 heat exposure of different types of people – pedestrians, cyclists, and fast-food workers or
81 traffic flaggers – is poorly documented [17]. In addition to highlighting how little we
82 understand about active travel and heat, models by Karner, Hondula, and Vanos [17] suggest
83 that low-income individuals and other vulnerable populations are more likely to rely on non-
84 motorized travel, increasing their potential heat exposure.

85 Thus far, there is little in the literature regarding the direct effects of the presence of
86 vehicles on microclimates and personal heat exposure. Lindberg et al. [18] identified waste
87 heat – released through fixed sources such as cooling and lighting as well as the
88 transportation system – as one of the factors affecting the outdoor thermal environment [18].
89 Thus, it is important to incorporate vehicular waste heat contributions to temperature changes
90 in urban areas. In addition, Hart & Sailor [19] demonstrated that TA near major roadways are
91 the warmest in the area due to the impervious nature of the roads and increased building and
92 waste heat emissions [19]. To date, few studies capture the direct effect of vehicular waste
93 heat on personal heat exposure. As Keith, Meerow, and Wagner [5] found, sixty percent of
94 heat planning research was published within the last five years, but the majority focuses on

95 modeling or mapping heat, suggesting that there is more to be explored through natural and
96 field experiments.

97 A notable exception to the understudied area of waste heat research in the field is
98 Grgis, Elariane, and Elrazik [20] who documented the range of temperature changes caused
99 by idling buses and domestic air conditioning condensers through the use of infrared cameras.
100 Air conditioners increased the TA by almost 1.0°C (1.8°F). Overall, the presence of idling
101 buses increased the surrounding TA from 1.0°C to 4.0°C (1.8°F to 7.2°F) due to the heat
102 emitted from idling buses and the associated reduction in air velocity [20]. While Grgis,
103 Elariane, and Elrazik [20] addresses the direct effect of large vehicles on TA, it does not
104 identify the effect on WBGT, a common way of identifying how various temperatures and
105 external factors such as wind and perspiration feel to the human body.

106 This pilot study explores the impact of traditional gasoline-powered vehicular waste
107 heat on the microclimates near vehicles – spaces that non-vehicular travelers often occupy.
108 Our research seeks to answer how the presence of traditional gas-fueled vehicles influences
109 personal heat exposure. This experiment was designed to quantify how much the presence of
110 a fleet of idling gasoline-fueled vehicles influences TA and personal heat exposure –
111 measured using WBGT – while controlling for several other factors in a covered parking
112 garage. This design includes two primary comparisons: (a) vehicles idling versus not idling
113 and (b) the presence (vehicle-adjacent) or absence (control) of vehicles. A study completed at
114 the University of Arizona's Point of Distribution (POD) for COVID-19 vaccinations in
115 Tucson, Arizona laid out the groundwork for the personal heat exposure methodology used in
116 the current study, such as instrumentation, type of data collected, and heat-risk metrics [21].
117 Another study following a similar methodology modified instrument placement and collected
118 TA, WBGT, wind speed, and traffic entry and exit data at the same Tucson POD, focusing on
119 sites 1.7-2.0 meters (5.5-6.5 feet) away from vehicular traffic at the three highest risk

120 locations [22]. This analysis suggested a vehicular waste heat effect, even though the
121 variation in heat measured was high due to natural experiment factors [22].

122 We hypothesized that the presence of vehicles would increase ambient air
123 temperatures (TA) and wet bulb globe temperatures (WBGT), increasing personal heat
124 exposure in nearby microclimates. This paper reports these findings, provides a framework
125 for future similar microclimate measurements, and identifies ways to understand and mitigate
126 vehicular waste heat effects on personal heat exposure.

127 **Materials and Methods**

128 **Study area and sites**

129 We collected data for this study in the University of Arizona (UArizona)'s South
130 Stadium Garage in Tucson, Arizona on June 4, 2022, from 8:00 AM through 10:00 AM. This
131 study expands on methodology reported from the UArizona COVID-19 vaccination POD in
132 April 2021 [21] and expands on experiment design ideas documented in a connected
133 presentation [22]. For this experiment, researchers blocked off the entrances to the first floor
134 of the South Stadium Garage and located the experiment in an area that would reduce
135 temperature variation from wind, other vehicles, and the sun.

136 We collected data using nine Kestrel 5400 devices located throughout the parking
137 garage. Fig 1 shows the location of the Kestrels and the vehicle fleet during data collection on
138 June 4, 2022. The vehicle fleet consisted of six Chevrolet Malibu vehicles, a type of mid-size
139 sedan, from the UArizona fleet. Five vehicles were 2020 models, and one was a 2019 model;
140 all were equipped with traditional gasoline-fueled engines. We used the dimensions of the
141 vehicles (approximately 4.9 meters by 1.8 meters [15 feet by 6 feet]) to create vehicle
142 location guidelines of 6.7 by 3.7 meters (22 feet by 12 feet) boxes, marked in Fig 1 in three
143 columns (columns 1, 2, and 3) and two rows (rows A and B) with additional buffer spaces.
144 These measurements are also shown in Fig 1.

145 **Fig1. Map of Site with Locations Marked**

146

147 Control Kestrels (West, West 2, and East) were placed away from the vehicle fleet,
148 but within the garage to maintain similar conditions, such as similar ground cover and
149 airflow. These three control Kestrels were set up to determine how effectively each Kestrel
150 acted as a control. Both West Kestrels are directly next to each other to check the accuracy of
151 the two instruments. They were accurate to one another, with the average difference between
152 the instruments recorded as 0.0056°C (0.01°F), with a standard deviation of 0.1°C (0.18°F),
153 giving us a measure of our instrument consistency. By reviewing wind roses and summary
154 statistics, we found that the west end of the garage was exposed to more inconsistent wind
155 speeds, while the east end had more similar microclimatic conditions to the vehicle test site.
156 Thus, when we refer to the control from this point on, we are referring to East Kestrel.

157 Tucson is in a semi-arid, desert environment characterized by low humidity and hot
158 temperatures during the early summer months. The Tucson International Airport recorded an
159 average June 2022 TA of 31.7°C (89.1°F) with 5.8 millimeters (0.23 inches) of precipitation
160 over the month [23]. On the morning of June 4th, the airport TA averaged 27.8°C (82.0°F)
161 between 7:00 AM and 9:20 AM, the time of active data collection [24]. This was slightly
162 lower than the Kestrel 5400 control on site, which recorded an average TA of 28.1°C
163 (82.5°F) at that same time. Average wind speed recorded at the airport was 9.7 kph (6.0
164 mph); the site's control Kestrel measured an average wind speed of 0.1 kph (0.07 mph).
165 There was no precipitation recorded on the data collection day.

166 **Data collection**

167 We used the Kestrel 5400 devices to collect ambient air temperature (TA), wet-bulb
168 globe temperature (WBGT), and wind speed for this analysis. Data was recorded once every
169 ten seconds during the study period.

170 Once we set up all Kestrels and vehicles (see Fig. 1), we waited 15 minutes to allow
171 the Kestrels to normalize to background temperatures and began our experiment at 7:15 AM.
172 Vehicles were then turned on at 7:35 AM (within approximately 15 seconds of each other).
173 Each vehicle had air conditioning set to its max value but was otherwise left idling for the
174 next 50 minutes. After 50 minutes had passed, the research team turned the vehicles off at
175 8:20 AM. Vehicles remained present, but with their engines off for the next hour. The
176 experiment ended at 9:20 AM. We call these three periods (a) Vehicles Off, (b) Vehicles On,
177 and (c) Cool Off, respectively throughout our analysis.

178 Full descriptive statistics for our data are provided in Table 1. Our descriptive
179 statistics demonstrate the averages and standard deviations for measurements collected using
180 the nine Kestrel 5400 instruments.

181 **Table 1 Descriptive Statistics of Data Collected**

| | | Vehicle-Adjacent Kestrels | | | | | | Control Kestrels | | |
|---|-----------------|---------------------------|-------|-------|-------|-------|-------|------------------|-------|-------|
| Location: | | 1A | 1B | 2A | 2B | 3A | 3B | East | West | West2 |
| Ambient Air Temperature (TA) (°C) | Mean | 28.30 | 28.33 | 28.30 | 28.29 | 28.26 | 28.14 | 28.04 | 27.70 | 27.71 |
| | St. Dev. | 0.89 | 0.79 | 0.77 | 0.77 | 0.73 | 0.71 | 0.68 | 0.90 | 0.89 |
| Wet Bulb Globe Temperature (WBGT) (°C) | Mean | 19.51 | 19.62 | 19.40 | 19.70 | 19.60 | 19.56 | 19.56 | 18.82 | NA |
| | St. Dev. | 0.50 | 0.43 | 0.40 | 0.44 | 0.37 | 0.36 | 0.35 | 0.56 | NA |
| Wind Speed (m/s) | Mean | 0.35 | 0.15 | 0.15 | 0.03 | 0.03 | 0.05 | 0.07 | 0.51 | 0.56 |
| | St. Dev. | 0.38 | 0.26 | 0.27 | 0.12 | 0.13 | 0.16 | 0.20 | 0.38 | 0.48 |
| Notes: Each Kestrel collected 751 observations, once every 10 seconds, summarized here. Each minute (with six 10-second observations) was averaged before the regression analysis was conducted. NA: Not available. | | | | | | | | | | |

182

183 **Analysis**

184 We downloaded Kestrel 5400 data as a .CSV file and imported into the statistical
185 programming software, R, for analysis. We analyzed data at the raw 10-second intervals and
186 at one-minute averages (e.g., averaging six 10-second observations), although only the results

187 for the minute averages were used in regression analysis in this paper. First, we examined the
188 temperature measurements graphically, paying attention to the general morning warming
189 temperature trend seen in the control and then comparing that trend with the vehicle-adjacent
190 observations.

191 Second, we tested our research hypothesis using an ordinary least-mean square (OLS)
192 linear regression. We created models for two different dependent variables: TA and WBGT,
193 segmenting the data by vehicle-adjacent observations and control observations, for a total of
194 four models. In this regression analysis, we control for wind speed (meters per second). We
195 also include two dummy variables for the “Vehicles On” and “Cool Off” time periods
196 (compared with the initial “Vehicles Off” base case). The clear linear warming trend
197 consistent with increasing morning temperatures (7:15AM-9:20AM) suggested we add time
198 elapsed as an independent variable instead of employing additional time series techniques.
199 For the vehicle-adjacent models, we also included a dummy variable for distance from
200 vehicle (Row A [closest, 1.5m or 5ft] = 0; Row B [furthest, 3.0m or 10ft] =1).

201 We expected to see a similarly identified vehicle effect in WBGT and in TA because
202 of the controlled effects of radiant heat and wind speed. We hypothesized that the anticipated
203 vehicle-caused heat in the surrounding area would be a result of waste heat; thus, these
204 changes would be equally captured in both measurements. During our tests, we expected to
205 see WBGT and TA significantly increase at a higher rate when vehicle engines were on, and
206 with the presence of vehicles. We anticipated this difference would be detected at a lagging
207 rate because WBGT is also slower to respond to changes in the environment due to the time it
208 takes for the interior of the bulb in the instrument to warm. We hypothesized that our control,
209 set up within the garage on the same paved ground cover, but at a slightly lower elevation due
210 to the subtle slope in the parking garage, would record consistently lower TA and WBGT.

211 **Results**

212 In this pilot study, we used Kestrel 5400 devices to document the potential waste heat
213 effects of a fleet of six gasoline-powered vehicles on the surrounding microclimate and
214 personal heat exposure by collecting TA, wind velocity, and WBGT. The results from the
215 four regressions are provided in Table 2 and explored further in this section. Explained
216 variation, or goodness-of-fit, was much higher for TA (control adjusted-R2: 0.982, vehicle-
217 adjacent: 0.944) than for WBGT (control adjusted-R2: 0.863, vehicle adjacent: 0.864). This is
218 likely because the WBGT measurement includes the radiant heat from both vehicles and the
219 built environment, the latter which is slower to respond to changes in microclimates than TA.
220

Table 2 Regression Results for Four Models of Ambient Air Temperature (A, B) and Wet Bulb Globe Temperature (C, D) at Two Locations (Control and Vehicle-Adjacent)

| Model: | A | | | B | | | C | | | D | | |
|---|------------------------------|---------------------|------------------|------------------------------|---------------------|------------------|---------------------------------|---------------------|------------------|---------------------------------|---------------------|------------------|
| Dependent variable: | Ambient Air Temperature (°C) | | | Ambient Air Temperature (°C) | | | Wet Bulb Globe Temperature (°C) | | | Wet Bulb Globe Temperature (°C) | | |
| Location | Vehicle-Adjacent | | | Control | | | Vehicle-Adjacent | | | Control | | |
| Independent Variables: | Coef | Confidence Interval | p-value | Coef | Confidence Interval | p-value | Coef | Confidence Interval | p-value | Coef | Confidence Interval | p-value |
| Intercept | 26.717 | 26.651 – 26.784 | <0.001 | 26.683 | 26.599 – 26.767 | <0.001 | 18.611 | 18.554 – 18.668 | <0.001 | 18.776 | 18.658 – 18.895 | <0.001 |
| Wind (m/s) | -0.053 | -0.115 – -0.009 | 0.094 | -0.095 | -0.205 – -0.015 | 0.09 | -0.173 | -0.226 – -0.120 | <0.001 | -0.452 | -0.606 – -0.297 | <0.001 |
| Kestrel Location | | | | | | | | | | | | |
| Row A (Closest) | Base Case | | | Base Case | | | Base Case | | | Base Case | | |
| Row B (Furthest) | -0.036 | -0.063 – -0.008 | 0.01 | | | | 0.107 | 0.084 – 0.130 | <0.001 | | | |
| Time Period | | | | | | | | | | | | |
| Vehicles Off | Base Case | | | Base Case | | | Base Case | | | Base Case | | |
| Vehicles On | 0.102 | 0.003 – 0.202 | 0.044 | 0.281 | 0.157 – 0.406 | <0.001 | 0.086 | 0.001 – 0.171 | 0.048 | 0.174 | -0.001 – 0.349 | 0.051 |
| Cool Off | 0.516 | 0.393 – 0.639 | <0.001 | -0.071 | -0.235 – -0.092 | 0.389 | 1.221 | 1.116 – 1.326 | <0.001 | 0.984 | 0.754 – 1.214 | <0.001 |
| Time Elapsed (T_elapsed) | 0.024 | 0.019 – 0.030 | <0.001 | 0.032 | 0.025 – 0.040 | <0.001 | 0.015 | 0.010 – 0.020 | <0.001 | 0.024 | 0.014 – 0.035 | <0.001 |
| Interacted Time Elapsed and Time Period | | | | | | | | | | | | |
| T_elapsed * Vehicles-Off | Base Case | | | Base Case | | | Base Case | | | Base Case | | |
| T_elapsed * Vehicles-On | 0.006 | 0.000 – -0.012 | 0.038 | -0.014 | -0.022 – -0.006 | 0.001 | 0.005 | -0.000 – -0.010 | 0.073 | -0.011 | -0.022 – -0.000 | 0.048 |
| T_elapsed * Cool-Off | -0.007 | -0.013 – -0.001 | 0.021 | -0.011 | -0.019 – -0.003 | 0.005 | -0.015 | -0.020 – -0.010 | <0.001 | -0.023 | -0.034 – -0.012 | <0.001 |
| Observations | 756 | | | 126 | | | 756 | | | 126 | | |
| Adjusted R2 | 0.944 | | | 0.982 | | | 0.864 | | | 0.863 | | |

Date of data collection: June 4th, 2022; **Site:** University of Arizona South Stadium Garage; **Unit of analysis:** one-minute average observations between 7:15 AM through 9:20 AM

p-value **bolded** when < 0.05

223 After we control for the location of the Kestrels and the idling engines, we found the
224 TA increased at a significant ($p < 0.001$) rate of 0.024°C and 0.032°C for the vehicle-adjacent
225 and control Kestrels, respectively, throughout the entire period of data collection. This can be
226 interpreted as the per minute temperature increase throughout the morning within the garage,
227 which we refer to as the background morning temperature. For WBGT, we found this
228 significant ($p < 0.001$) rate to be 0.015°C and 0.024°C for vehicle-adjacent and control
229 Kestrels, respectively. For the vehicle-adjacent Kestrels, the observations in “Row B” (3m)
230 observed statistically lower ambient temperatures (-0.036°C , $p < 0.05$) and higher WBGT
231 temperatures (0.107°C , $p < 0.001$) compared with the “Row A” (1.5m) Kestrels. This again
232 may suggest WBGT may pick up on the radiant temperatures from the idling/cooling vehicles
233 that do not impact TA. Given that WBGT is a more appropriate proxy for human thermal
234 comfort, this suggests that the impact of radiant heat from idling vehicles may be more
235 strongly felt by humans than observed by ambient temperature measurements. This may also
236 be attributed to radiant heat that may be reflecting off a wall on the north side of the
237 experimental area, just beyond Row B of Kestrels.

238 The primary purpose of this pilot study was to quantify the additional temperature
239 increase that vehicles emit as waste heat; this was measured by comparing the rate increase in
240 temperature during the Vehicles On and Cool Off time periods, compared with the initial
241 Vehicles Off time period. We compare these changes by both the time period dummy
242 variables as well as the interaction of these time periods with the minute-by-minute time
243 elapsed.

244 For the vehicle-adjacent Kestrel model (Table 2, Column A), when vehicles are idling
245 (from 7:35 AM to 8:20 AM), the TA was approximately 0.1°C ($p < 0.05$) greater than when
246 vehicles were off, in addition a significant increase in TA over time by 0.006°C per minute (p
247 < 0.05). During the “Cool Off” period, the vehicle-adjacent Kestrels measured a 0.516°C

248 increase in overall TA with a slightly lower increase in overall TA per minute compared to
249 the “Vehicle Off” period (-0.007°C, $p < 0.05$).

250 For WBGT at the vehicle-adjacent kestrel (model C), the Vehicles On period and
251 Cool Off period were 0.086°C ($p < 0.05$) and 1.221°C ($p < 0.001$) greater, respectively,
252 compared with the Vehicles Off period. The higher temperatures during the Cool Off period
253 may reflect the lagged effect of an aggregated index measure of temperature. When
254 interacting the time elapsed in minutes with the two time periods, the Vehicles On period
255 resulted in a 0.005 °C greater rate of change in WBGT over time with marginal significance
256 ($p < 0.1$). Additionally, the rate of change for the Cool Off period was 0.015°C less ($p <$
257 0.001) than the base case. Since the morning temperatures were still increasing by 9AM, this
258 suggests that the WBGT may not be as sensitive to changes in temperature as the aggregated
259 index nature of the variable would suggest. WBGT is less sensitive to change, particularly
260 without changes in direct radiation heat from the sun, strong winds, and humidity; we
261 designed the experiment to minimize these effects (e.g., block sun and wind via the parking
262 garage and selecting a day with low humidity). The greater increase in WBGT for vehicle-
263 adjacent Kestrel during the Cool Off suggests perhaps the increase in radiant temperature
264 from the vehicles after having been on resulted in slightly higher temperature impacts for
265 WBGT (compared with TA) during the Cool Off period.

266 When comparing the measurements at the control Kestrel for TA and WBGT (model
267 B and D), TA was significantly greater during the Vehicles On period by 0.28°C ($p < 0.001$)
268 and WBGT was marginally significantly greater by 0.17°C ($p < 0.1$) compared with the
269 initial Vehicles Off period. While there is no difference in TA between the Cool Off and the
270 initial Vehicles Off period, the WBGT was nearly 1.0°C warmer ($p < 0.001$) during the Cool
271 Off period. For both TA and WBGT at the control location, the rate of change in temperature
272 per minute was both significant and less during the Vehicles On period (TA: -0.01°C, p

273 <0.01; WBGT: -0.01°C, $p < 0.05$) and Cool Off periods (TA: -0.01°C, $p < 0.01$; WBGT: -
274 0.02°C, $p < 0.001$). Given that the East control used in this analysis was behind the idling
275 vehicles, albeit significantly farther than the vehicle-adjacent vehicles, it is feasible that the
276 increase in TA during the Vehicles On period may be a result of the exhaust from the
277 vehicles pointing in the direction of the control. Alternatively, the positive difference in
278 WBGT at the control location during the Cool Off—roughly 80% of that measured at the
279 vehicle-adjacent location—may have increased due to the radiant temperatures of the
280 vehicles measured at a further distance.

281 To depict the regression results graphically, we used each of the four models to
282 predict the average expected temperatures for from each of the four regressions assuming no
283 wind speed at the 1.5m (“Row A”) vehicle-adjacent location, and then we graphed these
284 results against the one-minute observations (see Figs. 2-5). We also observe some outliers in
285 the graphic towards the end of the collection period (after 9:00AM), particularly in the
286 WBGT models (Fig 4 and 5). We believe it is related to a slight increase in wind speed. We
287 selected this parking garage location because it was a semi-enclosed space to allow for
288 outdoor temperature increases while minimizing radiant heat from the rising sun as well as
289 wind. Wind speed is both marginally significant and negatively related to TA (models A and
290 B), and it is significantly and negatively related to WBGT (models C and D). The slightly
291 greater statistical significance and effect size for wind and WBGT is an expected result
292 because WBGT incorporates wind as well as humidity and radiation within the index
293 calculation. A one meter per second increase in wind speed leads to a 0.17°C drop in WBGT
294 in vehicle-adjacent Kestrels and a 0.45°C in WBGT in the control model.

295 **Fig 2. Average Ambient Air Temperature (in degrees F) Across Time for East Control**

296 **Fig 3 Average Ambient Air Temperature (in degrees F) Across Time for Vehicle-
297 Adjacent Kestrels**

298 **Fig 4. Average Wet Bulb Globe Temperature (in degrees F) Across Time for East**

299 **Control**

300 **Fig 5. Average Wet Bulb Globe Temperature (in degrees F) Across Time for Vehicle-**

301 **Adjacent Kestrels**

302 **Discussion and conclusion**

303 Overall, the impact of vehicles on transportation systems; the impact of transportation
304 systems to the UHI effect, microclimates, and personal heat exposure; and the interaction of
305 all of these on non-vehicular travel behavior is poorly understood. This pilot study
306 contributes to a better understanding of the relationships between gasoline-fueled vehicular
307 waste heat and microclimates immediately adjacent to idling vehicles using TA and WBGT.
308 Additionally, the experiment findings support our hypothesis that vehicle waste heat can
309 influence personal heat exposure within 1.5-3.0 meters of idling vehicles. This was
310 demonstrated most clearly in the vehicle-adjacent Kestrel by showing a TA increase of
311 0.006°C per minute for a total increase of 0.032°C per minute when the vehicles are on and
312 idling versus 0.024°C per minute increase that occurs from expected background morning
313 temperatures when the vehicles are off—roughly a 25% increase in the rate of change in
314 temperatures. Notably, the background morning temperatures for the control TA model show
315 a similar climb throughout (0.032°C per minute).

316 Our findings demonstrate that both vehicle presence and engine idling can increase
317 personal heat exposure and warrant further study. By understanding the influence of vehicles
318 on personal heat exposure at a human scale, we further inform design and operational
319 strategies to improve the experiences and heat safety of all travelers. For example, to avoid
320 excessive heat risk during warmer periods, signal timing may be reconfigured to prioritize
321 active travelers, minimizing time spent alongside idling vehicles at intersections or during
322 excessive idling periods, such as in construction. Another potential heat exposure solution to

323 help minimize the effects of vehicular waste heat would be cooling buffers, such as lining
324 walkways with trees. Additionally, understanding the cool-off period and conditions during
325 which it occurs would provide information on how elevated temperatures clear out in areas
326 such as intersections where traffic cycling occurs.

327 Our results also hint at some temporal questions. Results from this experiment
328 indicate that temperatures near idling vehicles steadily increase at a faster rate, approximately
329 25% greater in this morning's experiment. Although we arbitrarily cut the time to 50 minutes
330 for the six idling vehicles, our data showed no major signs of stagnation in the rate of
331 temperature increase. Extending the time in future studies could indicate if the rate remains
332 linear or has an asymptotic limit. This would inform situations involving idling cars for hours
333 at a time, such as ports-of-entry, drive-thru restaurants, heavy-traffic arterial roads, and more.
334 Testing other models of vehicles, including older vehicles and vehicles with larger engines,
335 could also help define the range of exposure associated with a fleet.

336 Personal heat exposure near an idling vehicle is a function of the time spent near the
337 idling vehicle and the length of time the vehicle – or vehicles before it in the same space –
338 has been idling. As a next step, we suggest a sensitivity analysis that uses these TA and
339 WBGT relationships to discover the point at which pedestrian and cyclist heat safety might
340 be of concern. For example, once WBGT exceeds 27°C (80.6°F), precautions should be taken
341 while completing moderate work, such as walking at 5.6 kph (3.5 mph, about average
342 walking speed) while carrying objects [25]. This threshold could be reached quickly while
343 walking to a bus stop with shopping bags near a congested intersection. Furthermore, to
344 better estimate the impact on human thermal comfort, more work is needed to understand at
345 what points heat impacts human psychological and physical systems for different people in
346 different conditions.

347 Finally, confirming the waste heat of gasonline-powered vehicles has implications for
348 our growing understanding of the UHI effect, given current vehicle fleet compositions. This
349 research demonstrates the contribution of waste heat to a microclimate, as shown by a fleet of
350 six cars powered by gasoline. A large city likely has hundreds of thousands of cars idling at
351 any one time, resulting in a significant additional UHI effect [11]. Transitioning to an electric
352 vehicle fleet or alternative modes of travel (e.g., biking, walking, transit) may reduce carbon
353 emissions and mitigate urban heat by reducing the personal heat exposure of individuals who
354 find themselves along roads with idling cars. Until that transition is complete, the waste heat
355 from vehicles into the surrounding thermal environment is a phenomenon for which planners
356 and engineers should account, plan, and mitigate.

357 By better understanding the relationship between waste heat and vehicle presence, we
358 can strengthen heat resilience efforts in cities through heat mitigation and management. Thus,
359 we recommend further research to document and understand personal heat exposure for
360 travelers across transportation modes and how vehicles contribute to increasing heat risk.

361 **References**

- 362 1. Intergovernmental Panel on Climate Change (IPCC). Climate change 2023: Synthesis
363 report. Contribution of Working Groups I, II and III to the Sixth Assessment Report of
364 the Intergovernmental Panel on Climate Change [Internet]. H. Lee, J. Romero, editors.
365 Intergovernmental Panel on Climate Change (IPCC); 2023. 35–115 p. Available from:
366 <https://doi.org/10.59327/IPCC/AR6-9789291691647>
- 367 2. US EPA. Climate Change Indicators: Heat Waves [Internet]. 2021 [cited 2022 Jul 30].
368 Available from: <https://www.epa.gov/climate-indicators/climate-change-indicators-heat->
369 waves
- 370 3. Lai D, Liu W, Gan T, Liu K, Chen Q. A review of mitigating strategies to improve the
371 thermal environment and thermal comfort in urban outdoor spaces. *Science of The Total
372 Environment*. 2019 Apr 15;661:337–53.
- 373 4. Chen L, Ng E. Outdoor thermal comfort and outdoor activities: A review of research in
374 the past decade. *Cities*. 2012 Apr 1;29(2):118–25.
- 375 5. Keith L, Meerow S, Wagner T. Planning for extreme heat: a review. *Journal of Extreme
376 Events*. *Journal of Extreme Events*. 2019;6(03n04):2050003.

377 6. Keith L, Meerow S. Planning for Urban Heat Resilience [Internet]. American Planning
378 Association; 2022 p. 100. (Planning Advisory Services (PAS) Report). Report No.: 600.
379 Available from: <https://www.planning.org/publications/report/9245695/>

380 7. Rizwan AM, Dennis LYC, Liu C. A review on the generation, determination and
381 mitigation of Urban Heat Island. *Journal of Environmental Sciences*. 2008 Jan
382 1;20(1):120–8.

383 8. Sailor DJ. 3.12 - Energy Buildings and Urban Environment. In: Pielke RA, editor.
384 Climate Vulnerability [Internet]. Oxford: Academic Press; 2013 [cited 2021 Jul 22]. p.
385 167–82. Available from:
386 <https://www.sciencedirect.com/science/article/pii/B978012384703400321X>

387 9. Jia S, Wang Y. Effect of heat mitigation strategies on thermal environment, thermal
388 comfort, and walkability: A case study in Hong Kong. *Building and Environment*. 2021
389 Aug 15;201:107988.

390 10. Madsen TL, Olesen B, Reid K. New methods for evaluation of the thermal environment
391 in automotive vehicles. Technical University of Denmark, Department of Civil
392 Engineering [Internet]. 1986 Jan 1 [cited 2021 Jul 22]; Available from:
393 <https://www.osti.gov/etdeweb/biblio/7141519>

394 11. Sailor DJ, Lu L. A top–down methodology for developing diurnal and seasonal
395 anthropogenic heating profiles for urban areas. *Atmospheric Environment*. 2004 Jun
396 1;38(17):2737–48.

397 12. Osama A, Albitar M, Sayed T, Bigazzi A. Determining If Walkability and Bikeability
398 Indices Reflect Pedestrian and Cyclist Safety. *Transportation Research Record: Journal*
399 of the Transportation Research Board. 2020;2674(9):767–75.

400 13. Adkins A, Dill J, Luhr G, Neal M. Unpacking Walkability: Testing the Influence of
401 Urban Design Features on Perceptions of Walking Environment Attractiveness. *Journal*
402 of *Urban Design*. 2012;17(4):499–510.

403 14. Liu Z, Cheng KY, He Y, Jim CY, Brown RD, Shi Y, et al. Microclimatic measurements
404 in tropical cities: Systematic review and proposed guidelines. *Building and*
405 *Environment*. 2022 Aug 15;222:109411.

406 15. Hoffman JS, Shandas V, Pendleton N. The effects of historical housing policies on
407 resident exposure to intra-urban heat: a study of 108 US urban areas. *Climate*.
408 2020;8(1):12.

409 16. Wilson B. Urban heat management and the legacy of redlining. *Journal of the American*
410 *Planning Association*. 2020;86(4):443–57.

411 17. Karner A, Hondula DM, Vanos JK. Heat exposure during non-motorized travel:
412 Implications for transportation policy under climate change. *Journal of Transport &*
413 *Health*. 2015 Dec 1;2(4):451–9.

414 18. Lindberg F, Grimmond CSB, Yugeswaran N, Kotthaus S, Allen L. Impact of city
415 changes and weather on anthropogenic heat flux in Europe 1995–2015. *Urban Climate*.
416 2013 Jul 1;4:1–15.

417 19. Hart MA, Sailor DJ. Quantifying the influence of land-use and surface characteristics on
418 spatial variability in the urban heat island. *Theor Appl Climatol*. 2009 Mar 1;95(3):397–
419 406.

420 20. Girgis N, Elariane S, Elrazik MA. Evaluation of Heat Exhausts Impacts on Pedestrian
421 Thermal Comfort. Sustainable Cities and Society [Internet]. 2016 Nov [cited 2021 Jul
422 22];27. Available from: <https://trid.trb.org/View/1488375>

423 21. Keith L, Iroz-Elardo N, Austof E, Sami I, Arora M. Extreme heat at outdoor COVID-19
424 vaccination sites. *J Clim Chang Health*. 2021 Oct;4:100043.

425 22. Avila A, Iroz-Elardo N, Keith L, Currans K. Investigating the Influence of Running
426 Vehicles on Personal Heat Exposure at Outdoor COVID-19 Vaccination Sites. [Student
427 Scholar Presentation]. In: Annual Meeting of the Transportation Research Board.
428 Washington, D.C.; 2022.

429 23. National Climatic Data Center. Global Summary of the Month Station Details:
430 TUCSON INTERNATIONAL AIRPORT, AZ US, GHCND:USW00023160 | Climate
431 Data Online (CDO) [Internet]. [cited 2022 Jul 30]. Available from:
432 [https://www.ncdc.noaa.gov/cdo-](https://www.ncdc.noaa.gov/cdo-web/datasets/GSOM/stations/GHCND:USW00023160/detail)
433 [web/datasets/GSOM/stations/GHCND:USW00023160/detail](https://www.ncdc.noaa.gov/cdo-web/datasets/GSOM/stations/GHCND:USW00023160/detail)

434 24. University of Utah. MesoWest [Internet]. KTUS Data. [cited 2022 Jul 30]. Available
435 from: [https://mesowest.utah.edu/cgi-](https://mesowest.utah.edu/cgi-bin/droman/download_api2.cgi?stn=KTUS&hour1=13&min1=49&timetype=GMT&unit=0&graph=0)
436 [bin/droman/download_api2.cgi?stn=KTUS&hour1=13&min1=49&timetype=GMT&unit=0&graph=0](https://mesowest.utah.edu/cgi-bin/droman/download_api2.cgi?stn=KTUS&hour1=13&min1=49&timetype=GMT&unit=0&graph=0)

438 25. Departments of The Army, The Navy, and The Air Force. Occupational and
439 Environmental Healthy: Prevention, Treatment, and Control of Heat Injury. Technical
440 Bulletin MED No. 507. 1980: 1-21. In.

441

Attribution: Google Earth Pro 7.3.6.9345 (64-bit). (Dec. 12, 2019). South Stadium Garage, Tucson, AZ USA. 32°13'37.11"N, 110°56'45.41"W, Eye alt 453 ft. Borders and labels; road layers.
<http://www.google.com/earth/index.html> (Accessed March 2, 2023)

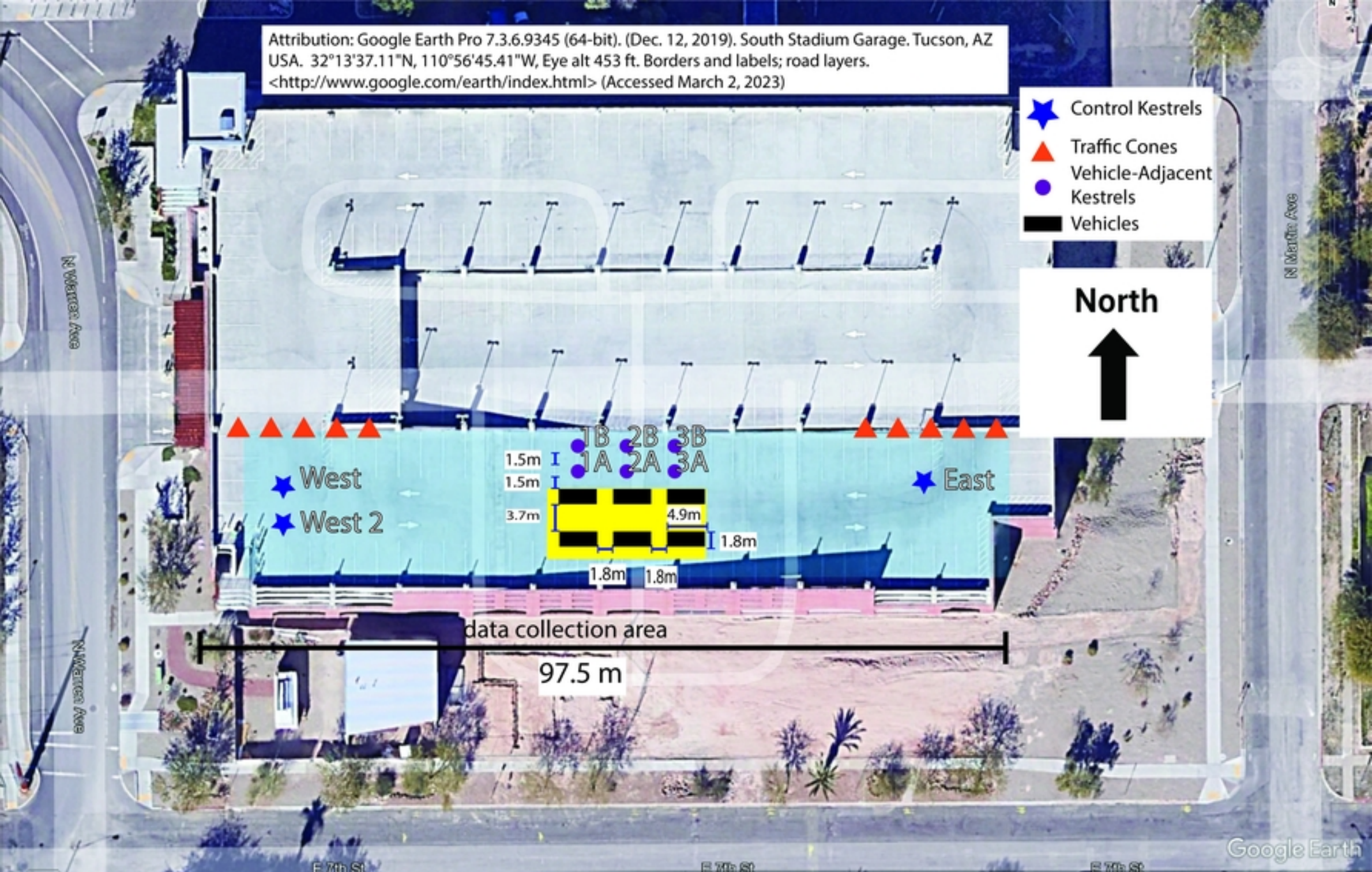


Fig 1

Average Ambient Air Temperature (Celsius) Across Time for Control Kestrel

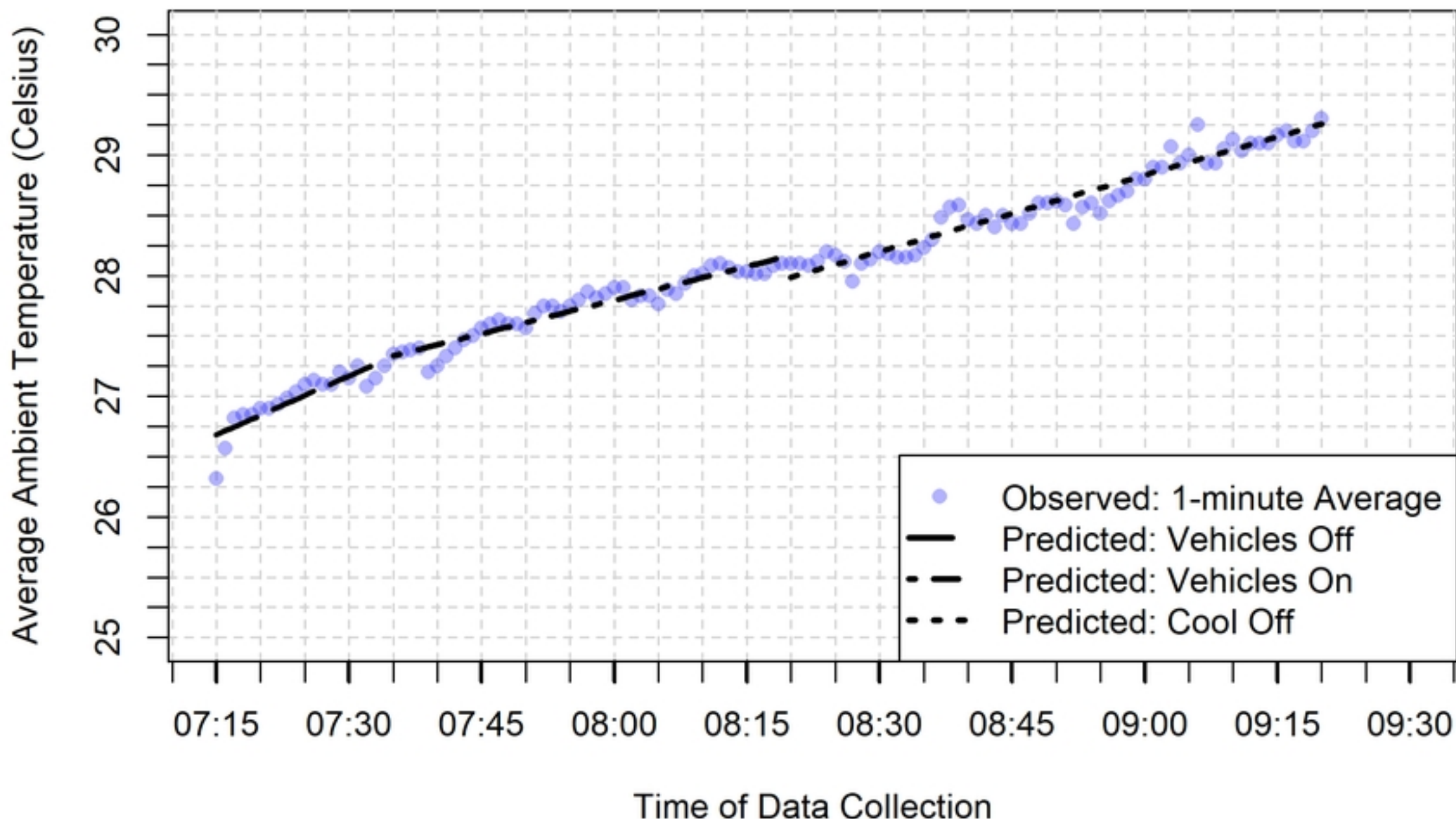


Fig 2

Average Ambient Air Temperature (Celsius) Across Time for Vehicle-Adjacent Kestrels

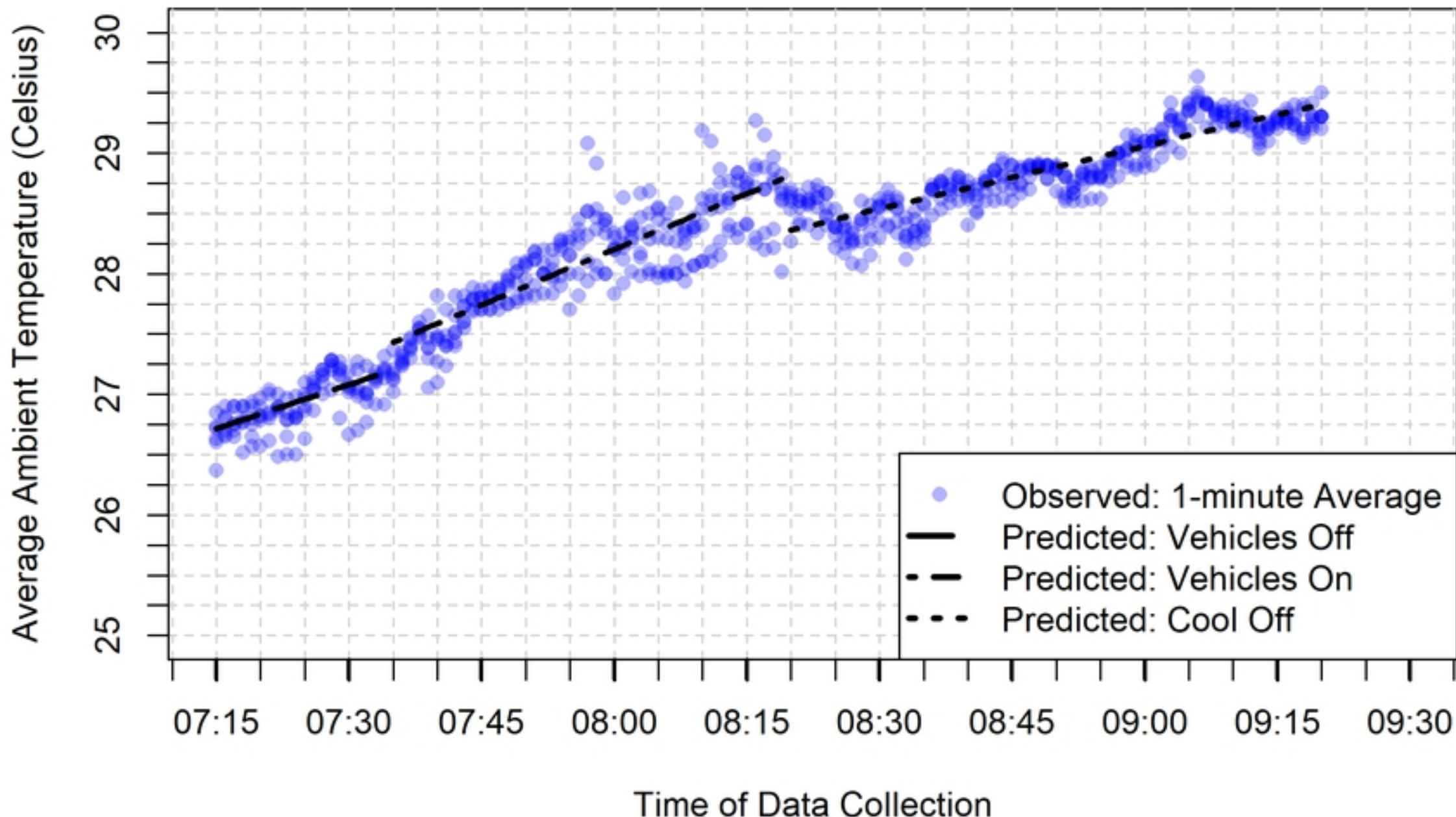


Fig 3

Average WBGT (Celsius) Across Time for Control Kestrel

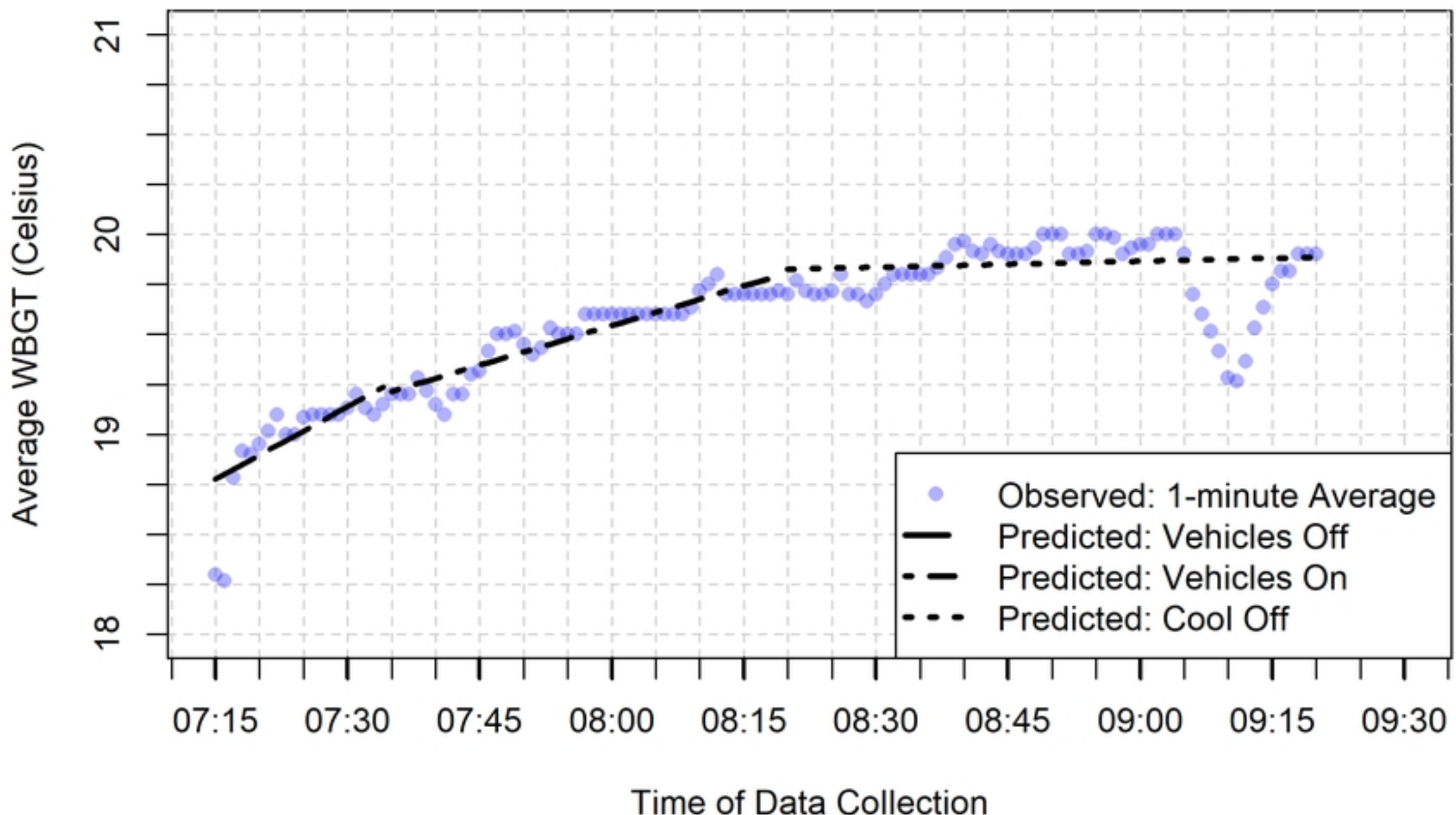


Fig 4

Average WBGT (Celsius) Across Time for Vehicle-Adjacent Kestrels

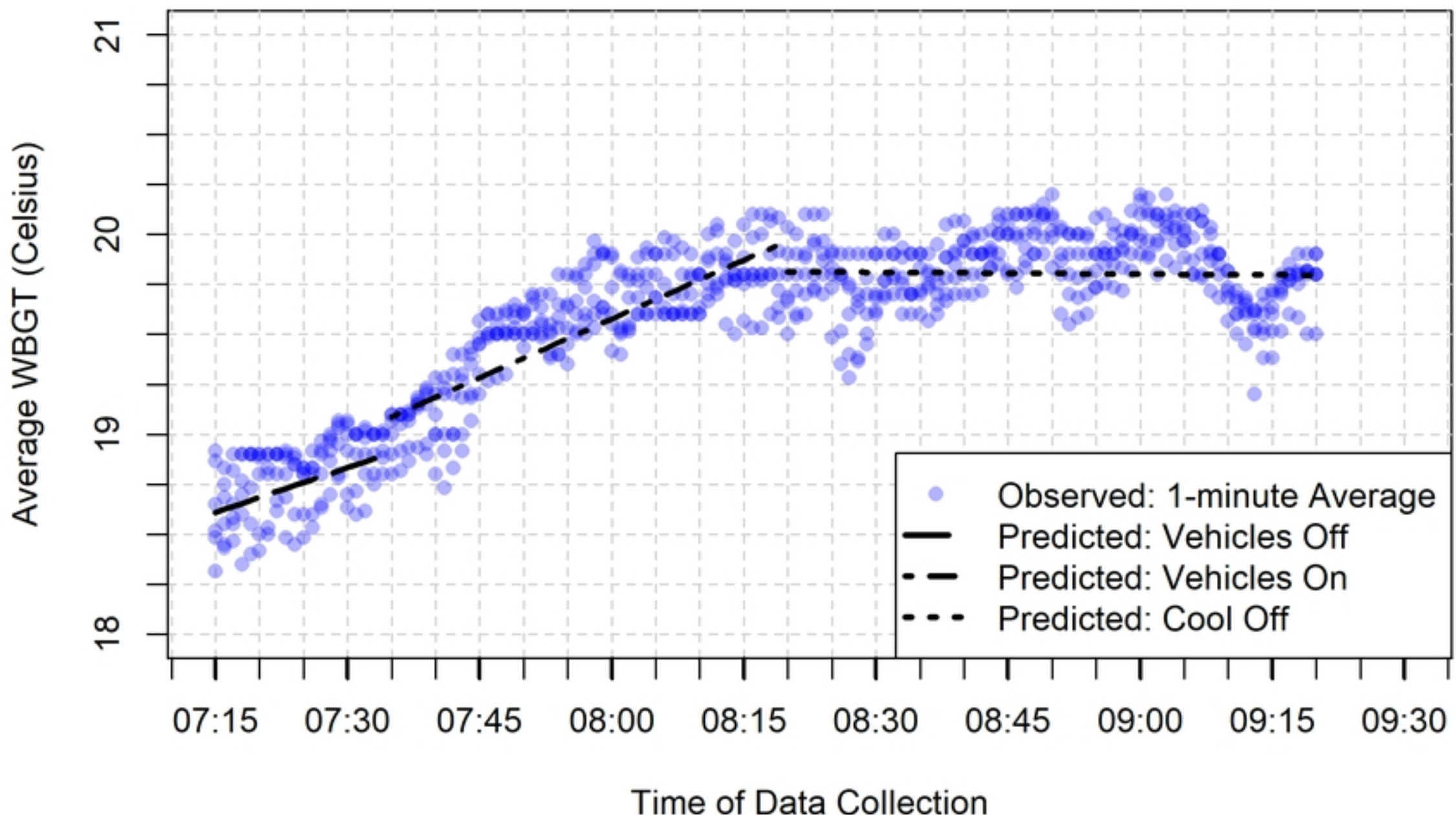


Fig 5